A Carbon Fibre Swingarm Design

B. Smith[a] and F. Kienhöfer[b]

Received 17 June 2014, in revised form 5 January 2015 and accepted 13 January 2015

The use of carbon fibre composites in structural automotive components such as swingarms is underdeveloped. Carbon fibre composites possess higher stiffness to weight ratios than commonly used automotive materials such as steel, aluminium and magnesium. In this study a novel prototype carbon fibre swingarm is presented. The vertical and torsional stiffness values of the prototype were measured to be 500 kN/m and 550 Nm/deg respectively. The prototype vertical stiffness is of an order of magnitude greater than the rear suspension stiffness (a deemed satisfactory minimum). The torsional stiffness of 550 Nm/deg is comparable to published values. The prototype carbon fibre swingarm is 1.5 kg lighter than its aluminium counterpart: a weight saving of 29%. A finite element (FE) model was developed which will be used to further reduce the weight of the swingarm. Validating the FE model using strain gauges produced mixed results. The finite element analysis (FEA) showed good correlation with the vertical displacement of the swingarm and reasonable correlation with the torsional deflection. The study illustrates the superior stiffness to weight ratio of carbon fibre (an important feature in its growing use in automotive component manufacturing) and the importance of validating FE models using macro-measurements (e.g. deflection) when dealing with complex composite structures which have ply overlap and high strain gradients.

Additional keywords: Swingarm, carbon fibre, FEA, strain measurements, ply overlap

Nomenclature

Roman

E_1	Young's modulus in the fibre or longitudinal direction
E_2	Young's modulus in the transverse direction
F_x	lateral tyre force
g	gravitational constant
G_{12}	modulus of rigidity
m	mass of the motorcycle
r	radius of turn
R_y	vertical reaction
t	width of tyre or thickness of laminate
v	longitudinal velocity of the motorcycle

Greek

υ_{12}	major Poisson's ratio

Abbreviations

FE	Finite Element
FEA	Finite Element Analysis

a. School of Mechanical, Industrial, and Aeronautical Engineering, University of the Witwatersrand; bevan.smith@wits.ac.za; Private Bag 3, Wits, 2050

b. SAIMechE member, School of Mechanical, Industrial, and Aeronautical Engineering, University of the Witwatersrand; frank.kienhofer@wits.ac.za

1 Introduction

Carbon fibre composites are a proven material choice for cosmetic, non-structural automotive parts[1]. While a 40-50% weight saving has been suggested[2] to be possible for automotive body panel applications and a 50% weight reduction for a suspension strut[3], the use of carbon fibre for load-bearing automotive components is still in its infancy. Carbon fibre composites possess higher stiffness to weight ratios than other commonly used automotive materials such as steel, aluminium and magnesium. In spite of this advantage, a limited number of studies have investigated designing and manufacturing composite swingarms[4,5,6]. These studies have either not reported the stiffness of the designed swingarm[4] or not experimentally measured the stiffness, relying on finite element analyses (FEA)[5,6].

In the design of swingarms, the stiffness plays a critical role in the motorcycle response and stability, i.e. the response time during cornering and the motorcycle weave mode stability are affected. It is important therefore to determine the swingarm stiffness characteristics that would give the designer insight into how the motorcycle might respond.

In this study, the first step in the redesign of a Ducati 1098 swingarm (originally made of aluminium) using carbon fibre composite is presented. The fibre layup and the manufacturing were not part of this investigation. The stiffness values were determined by experimentally measuring the vertical and torsional deflections of the prototype carbon fibre swingarm subjected to a range of loading conditions. The literature shows that finite element (FE) models have been developed for carbon fibre swingarms. A FE model of the swingarm was therefore developed to compare the results from this study to the two results published in the literature. The FE model will be used for future work to optimise the carbon fibre lay-up. This paper further discusses the effects that ply overlap have on the validity of the FE model. A greater degree of confidence in the FE model and insight into the FE model limitations are obtained through the conducted experimental testing.

2 Literature Review

The motorcycle swingarm is a key component of the rear suspension of a motorcycle. It connects the rear wheel of the motorcycle to the main chassis and it regulates the rear wheel-road interactions via the spring and shock absorber[7]. Two basic designs exist, namely the single-sided and double-sided swingarms. The single-sided swingarm has the benefit of allowing for easier removal of the rear wheel during racing. The disadvantage is that due to the asymmetry, a twisting moment acts in the arm which does not exist in a double-sided swingarm[6]. To maintain rigidity for a single-sided swingarm, extra material may be required which increases the unsprung mass of the rear side of the motorcycle. This is unfavourable because a higher unsprung mass decreases the roadholding of the rear wheel. The vertical stiffness can affect the motorcycle setup and

 © SAIMechE All rights reserved.

produce unpredictable behaviour if not rigid enough[8]. The aim is to maximise the vertical stiffness and ensure it is considerably higher than the rear suspension spring stiffness. The lateral and torsional stiffness affect the motorcycle response during cornering and the motorcycle weave mode[9]. The weave mode is the side to side movement of the rear of the motorcycle caused by the roll and yaw motion of the motorcycle. In general, it is desirable to maximise the swingarm lateral and torsional stiffness to reduce this instability. This initial step of designing the carbon fibre swingarm was to determine the stiffness characteristics and compare them with values obtained from other research. Furthermore, the weight of the prototype swingarm was compared with the original aluminium specimen.

Armentani *et al.*[10] compared the stiffness values of three different aluminium double-sided swingarms by carrying out both experimental tests and FEA. They stated that the main difficulty in designing a swingarm is to obtain the right balance between the flexional (lateral) and torsional stiffness. Loads acting on the rear wheel during cornering were defined as follows. When viewed from the rear of the motorcycle along the longitudinal axis (figure 1), the moment about the tyre contact point caused by the centrifugal or inertial force, mv^2/r, (that tends to restore the motorcycle to the vertical position) is balanced by the moment caused by the weight of the motorcycle and rider, mg, (that tends to cause the motorcycle to fall over).

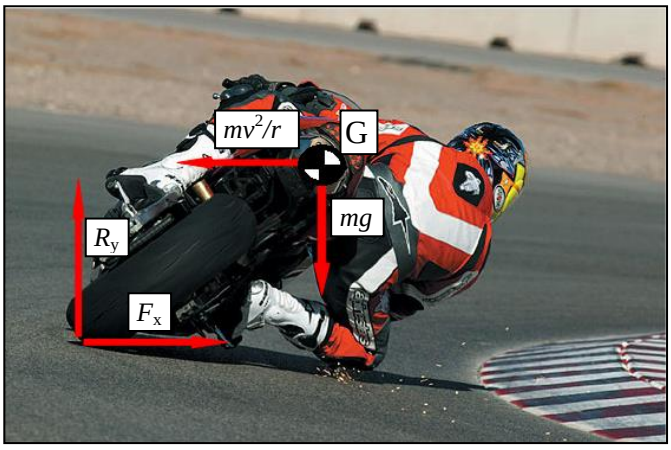


Figure 1: Loads acting on the swingarm during cornering[5]

Assuming that the wheels are thin, the resultant of these two forces is balanced by a vertical reaction, R_y, and lateral tyre force, F_x, at the wheel-road contact point and acts along the plane of the wheel. In reality however, due to the thickness of the tyres, t, the resultant force does not act in the plane of the wheel but along the line connecting the centre of mass and the tyre contact point (figure 2).

The actual resultant force has components acting parallel and perpendicular to the wheel plane. The perpendicular component will generate both a lateral force and a moment about the longitudinal axis. For a motorcycle with a mass of 230 kg, the moment was calculated by Armentani *et al.*[10] to be 31 Nm which was applied during experimental testing and FEA.

The torsional loading was measured as shown in figure 3. In their experimental setup, there was no spacer and spindle inserted between the wheel connection points to simulate real life conditions. By applying the load only on one arm without the spacer in between, it is most likely that higher displacements were measured (and consequently lower stiffness values) than if the spacer was inserted to simulate real life conditions. By applying the loads in this manner, torsional stiffness values of 102.9 Nm/deg, 140.8 Nm/deg and 140.8 Nm/deg were calculated respectively for the three motorcycle swingarms.

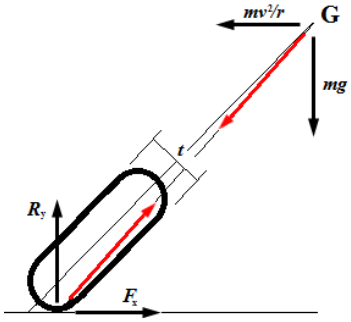


Figure 2: Loads acting on swingarm during cornering assuming thick wheels[10]

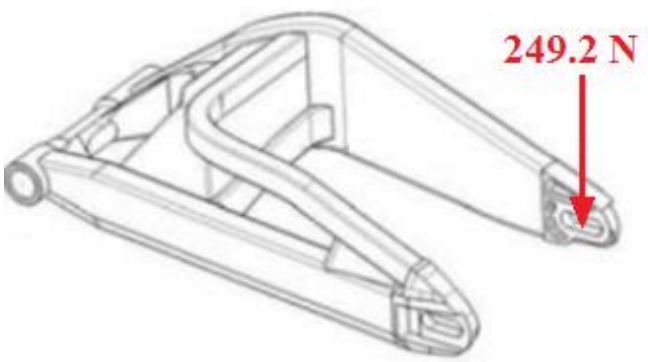


Figure 3: Torsional loading without the use of spacer and spindle[10]

Based on the above argument, the torsional stiffness values calculated by Armentani *et al.*[10] are assumed to be lower than the values that would be measured while simulating real life conditions. It will be seen later that the torsional stiffness values are indeed much lower than other values measured in the literature.

Risitano *et al.*[7] aimed to link objective data such as swingarm stiffness and natural frequencies with subjective information such as handling and comfort perceived by riders. They claimed that to characterize the swingarm it is important to look at the torsional stiffness. The more flexible the swingarm is the heavier the motorcycle feels to the driver and the more difficult manoeuvring becomes. The stiffer the swingarm, the quicker the response is during cornering. Risitano *et al.*[7] tested the torsional rigidity and symmetrical behaviour of three double-sided aluminium swingarms. The range of torsional loads was between 0 Nm and 400 Nm and torsional stiffness values of 670 Nm/deg, 890 Nm/deg and 1330 Nm/deg were calculated. FEA was also carried out on the swingarms and an average difference of 4% was found between experimental and simulated results.

Cossalter *et al.*[9] studied the effect the swingarm has on the weave mode stability of a 150 cc scooter. At

approximately 16 m/s (58 km/h) and higher the rigidity of the swingarm begins to affect the weave stability. They found that the more rigid the swingarm is in both torsional and lateral directions, the more stable the motorcycle is in terms of weave stability. This holds true only up until approximately 130 km/h above which an increase in lateral stiffness begins to decrease the weave mode stability.

Lake *et al.*[11] state that it is obvious that increasing swingarm torsional stiffness increases the weave mode stability but asked: what are acceptable values of swingarm torsional stiffness? Sharp[12] claimed a value of 209 Nm/deg would approach an absolutely rigid swingarm. Cossalter[13] however, stated that modern swingarms have values between 1000 Nm/deg and 2000 Nm/deg and Risitano *et al.*[7] (discussed above), measured values of 670 Nm/deg and higher. Armentani *et al.*[10] (also discussed above), measured values of between 102.9 Nm/deg and 140.8 Nm/deg which are unusually low when compared to other swingarms. The explanation for the low stiffness was discussed earlier. Lake *et al.*[11] concluded that the reported torsional stiffness values on contemporary swingarm designs are not consistent.

In terms of vertical loading, no literature was found that applied static vertical loads to a swingarm to determine the vertical stiffness. Consequently, the Leyni Durability Test used by Gaiani[14] was considered for vertical loading. The Leyni Test Rig is a durability rig which consists of a rotating drum with a 300 mm high step. The rear wheel of a motorcycle is mounted on a drum and as the drum rotates (with a speed of 3.7 Hz) it applies an impulse load to the wheel every time the step passes. During the cyclic loading, the initial static load due to the driver and passenger is 1960 N and a maximum dynamic applied loading of 5900 N occurs when the step impacts the wheel. In this study, vertical loads similar in magnitude to those applied during the Leyni Test have been used.

Although materials that are light and have high strength and rigidity have been used for swingarms such as aluminium[4] and magnesium alloy[15], carbon fibre composite has the benefit of allowing the designer to modify the material characteristics and structural stiffness[6] and has a higher stiffness to weight ratio[16]. Dragoni[5], Airoldi *et al.*[6] and O'Dea[4] carried out designs of swingarms using composite materials. Airoldi *et al.*[6] carried out a redesign of a single-sided swingarm using carbon fibre composite. Their goal was to compare a composite swingarm design with an existing aluminium design and to minimise the torsional, lateral and vertical deflections and mass by investigating the stacking sequences of the plies. O'Dea redesigned and manufactured a double-sided swingarm from a Honda CRF450 by moulding metal inserts into a carbon fibre epoxy composite.

The literature shows that there is an inconsistent range of torsional rigidity values quoted for swingarms, and no vertical stiffness values have been published. The few studies on composite swingarms have not addressed the difficulty of validating the FEA of such a complex composite structure with experimental testing.

3 Methodology: Experimental Setup

The goal of the experimental tests was to measure deflections and strains under various loads for the following purposes: (1) to determine the stiffness characteristics and strain distribution on the carbon fibre swingarm (figure 4) and (2) to use the experimental results to validate the FE model of the swingarm. Deflections and strains were measured while vertical and torsional loads were applied to the swingarm mounted on the test rig (figure 5). Although the forces acting on the swingarm are important from a structural point of view, the aim in this study was not to load the swingarm to failure but primarily to obtain stiffness and strain curves.

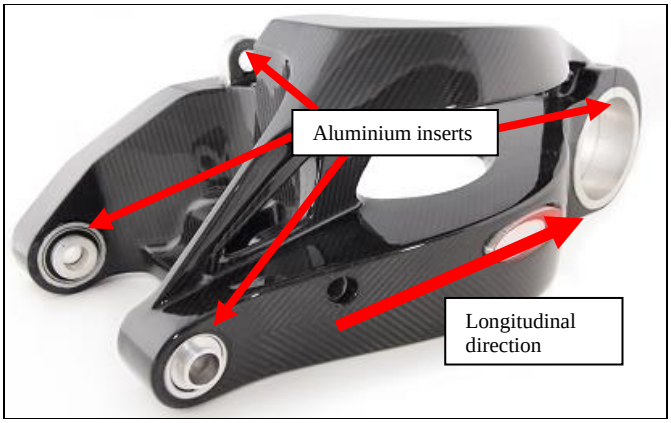


Figure 4: Carbon fibre swingarm

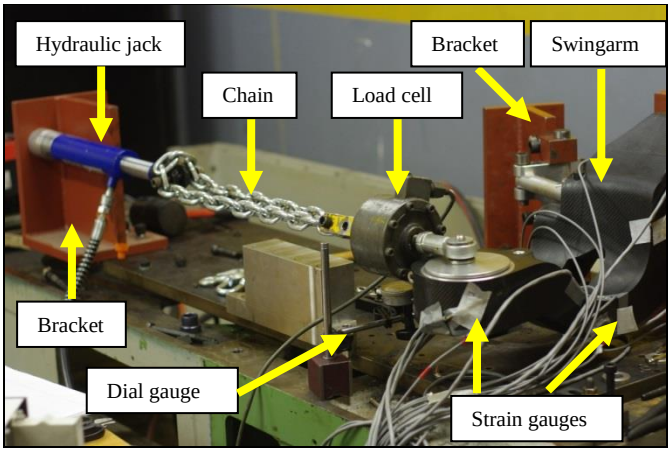


Figure 5: Test rig showing various components used during testing

3.1 Vertical loading

Figure 6 shows the rig setup to simulate vertical loading. Due to the design of the test rig, the swingarm was rotated 90° so that the vertical load was applied in the horizontal plane. The range of loads (based on the Leyni Test) applied to the swingarm was between 0 N and 8000 N in increments of 1000 N and was applied via a hydraulic jack. The load cell weight is of two orders of magnitude less than the applied forces, acts perpendicular to the applied forces and can therefore be neglected. Strains at eight positions on the swingarm (discussed later) were measured at each load increment. The vertical deflection at the wheel mount was measured using a dial gauge.

3.2 Torsional loading

The test rig was modified in order to apply a torsional load to the swingarm. The line of action of the force applied by

the jack was raised approximately 340 mm to create a moment arm about the longitudinal axis of the swingarm (figure 7). Due to the jack applying a force a distance away from the longitudinal axis of the swingarm, the effect is that a force and couple moment act at the wheel mount (figure 8). The magnitude of the moments applied to the swingarm was based on Risitano *et al.*[7] with the range being between 0 Nm and 680 Nm in increments of 34 Nm.

Strain and deflection was measured during the torsional loading. Deflections were measured at the wheel mount (Dial gauge 1) and at the position of load application (Dial gauge 2) (figure 8). The two deflection measurements allowed for calculating the rotational angle based on the moment.

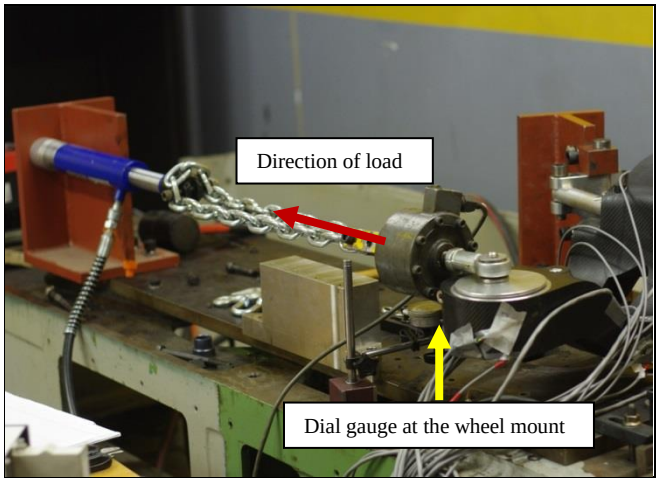


Figure 6: Simulated vertical loading of swingarm

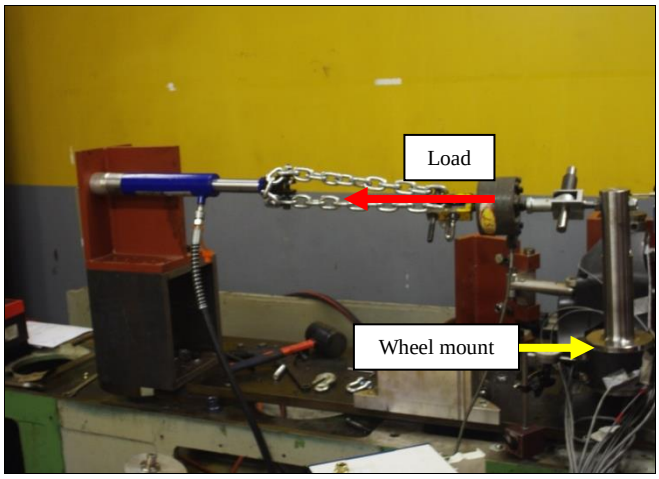


Figure 7: Torsional loading of swingarm

3.3 Position of strain gauges

Rosette strain gauges were mounted at eight positions on the swingarm (figures 9 and 10) to measure longitudinal and transverse strain. The swingarm was designed such that the longitudinal fibre directions were aligned with the swingarm longitudinal direction. The longitudinal strain gauge direction was aligned with the swingarm longitudinal direction and the longitudinal fibre direction. The transverse direction was perpendicular to the longitudinal gauge direction and parallel to the surface the gauge was placed on.

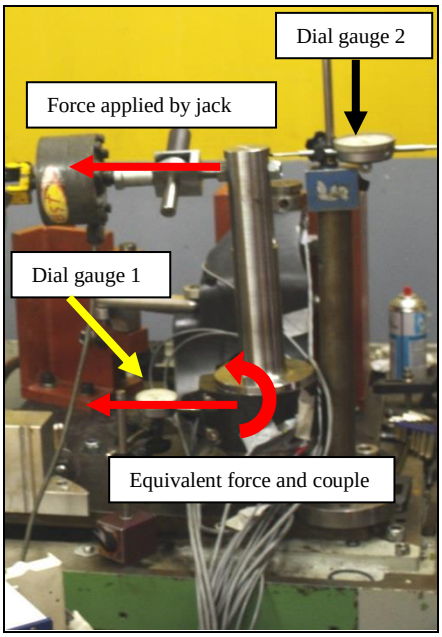


Figure 8: Test rig for torsional loading

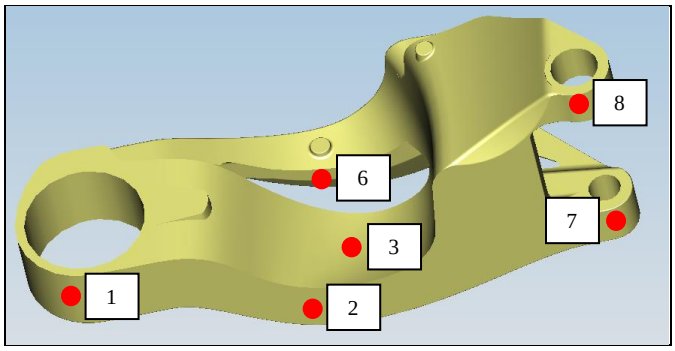


Figure 9: Strain gauge positions

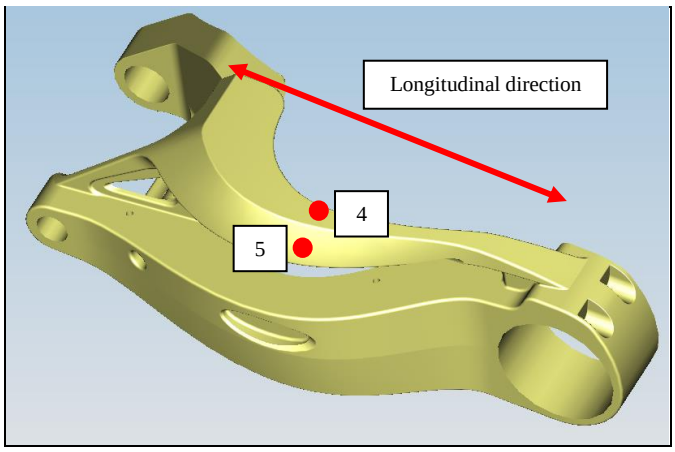


Figure 10: Strain gauge positions

4 Methodology: FE model

To develop the FE model, it was necessary to first determine the various zones on the swingarm and the type of layup that made up each zone[1]. Once that information was obtained, the following initial assumptions were made:

[1] A region on the swingarm with a specific type of fibre layup.

 © SAIMechE All rights reserved.

- Not all the zones would be modelled but only what was regarded as the most significant ones. The smaller zones with slight differences in layup would be included in the major layup surrounding it.
- Lamina (ply) overlap would not be modelled. To get a working FE model, the very complex modelling of the lamina overlap was ignored. Overlap occurs mainly in the corners where two different layups meet and due to the complexity of the swingarm, the overlap was disregarded.
- The aluminium inserts (figure 4) were not modelled so as to simplify the FE model. Loads and constraints acting at the aluminium inserts were averaged over the contact area between the aluminium and carbon fibre material.

The fibre layup consisted of a number of unidirectional and woven carbon fibre plies. The material properties were not explicitly known and therefore standard properties for both the unidirectional and woven plies were assumed which are presented in table 1. The approximate thickness, *t*, of each ply is also given.

Table 1: Material properties of the carbon fibre plies[17]

Material	E_1 (GPa)	E_2 (GPa)	G_{12} (GPa)	v_{12}[2]	t (mm)
Unidirectional	135	10	5	0.3	0.3
Woven	70	70	10	0.1	0.38

The FE model (figure 11) was subjected to the same loading conditions as the experimental testing. ANSYS Composite PrepPost was used to create the lay-ups for each area of the swingarm. ANSYS Static Structural was used to solve for and process results.

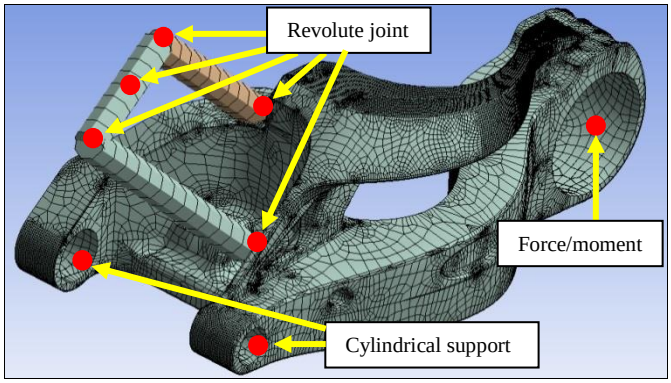


Figure 11: FE model of the swingarm including the rocker

The constraints on the FE model were based on the constraints placed on the swingarm when mounted to the test rig. Figure 12 shows the boundary conditions on the swingarm. The swingarm has six points of constraint (including the rocker arm) and one load application point (at the wheel mount). The constraints are made up of the pivot points and the rocker arm assembly. The pivot points are where the swingarm rotates about an axle which simulates being connected to the main chassis. The swingarm is also connected to rigid links simulating the rocker arm suspension. The load is applied at the wheel mount.

[2] Major Poisson's ratio.

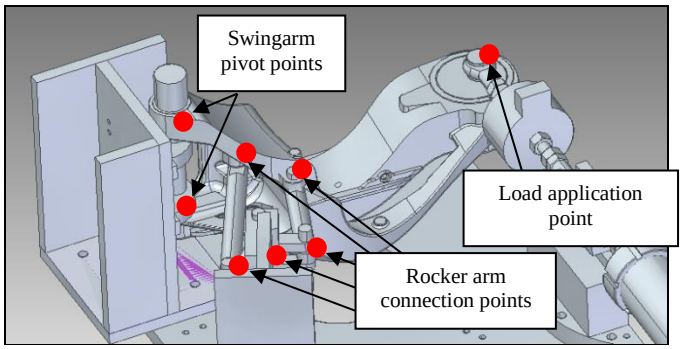


Figure 12: Boundary conditions of swingarm

The pivot points were modelled as cylindrical supports which allow only rotation about the axis passing through the pivots. For the rocker arm, revolute joints were used and for the load application point, forces and moments were applied to the surface of the wheel mount (figure 11).

4.1 Vertical testing

The FE model was assumed to be linear and during vertical loading (figure 13) only the maximum load of 8000 N was applied. The FE strains and deflections at maximum loading were calculated and intermediate results calculated using linearity.

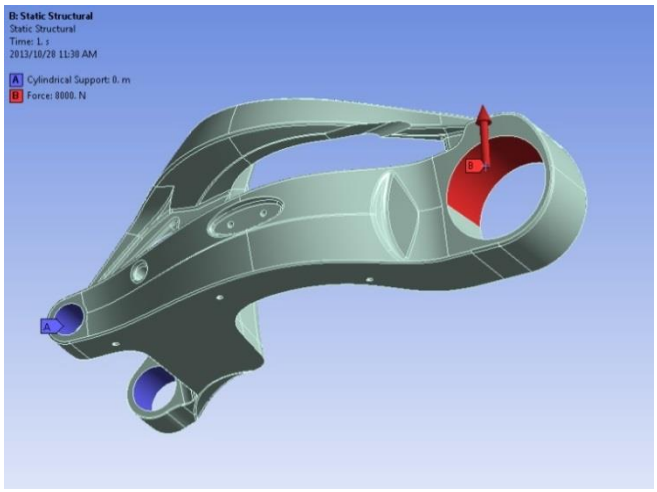


Figure 13: Vertical loading of FE model of swingarm

4.2 Torsional testing

Similarly, only the maximum moment of 680 Nm (with corresponding force) was applied to the FE model to simulate torsional loading (figure 14). Linear curves were generated for deflection and strain and compared with experimental results.

5 Experimental results and discussion

The aim of measuring deflection in the vertical and torsional directions was first to obtain the vertical and torsional stiffness values respectively. Once obtained, comparisons could be made with stiffness values found in the literature.

5.1 Vertical stiffness

The vertical stiffness value was calculated as 500 kN/m (figure 15). No comparison could be made because no literature was found that measured vertical swingarm stiffness. However, this value was concluded to be

sufficiently high to not negatively influence the effective vertical stiffness between the chassis and wheel. Typical spring stiffness values are in the region of 50 kN/m and 100kN/m and the combination of the swingarm and the rear spring will result in the rear spring stiffness being the dominating stiffness.

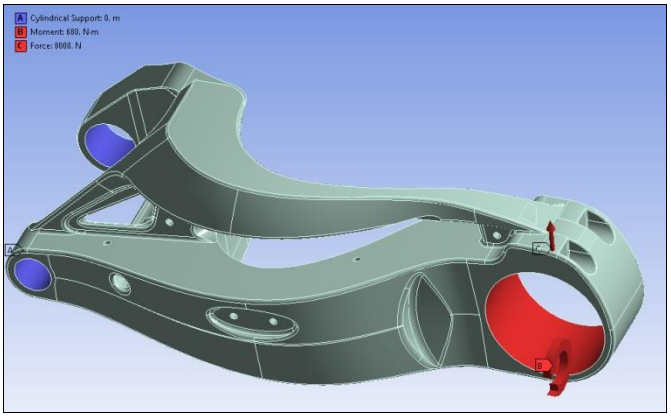


Figure 14: Torsional loading of FE model of swingarm

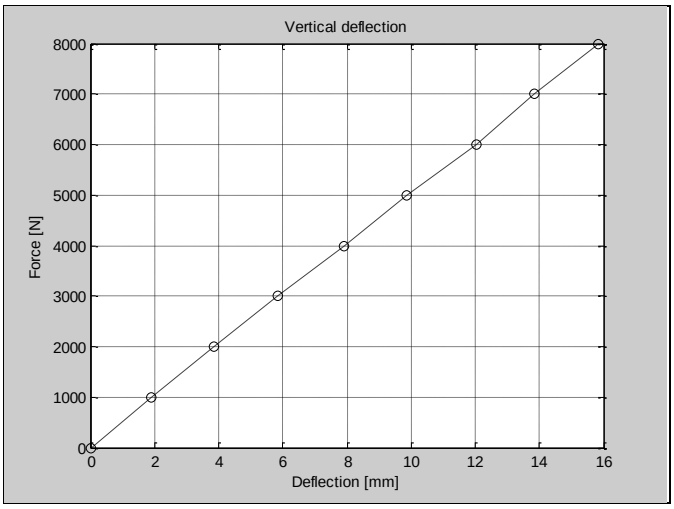


Figure 15: Vertical deflection curve showing the stiffness value of 500 kN/m

5.2 Torsional stiffness

The torsional stiffness was calculated as 550 Nm/deg (figure 16) and was found to be approximately in the middle of the spectrum of torsional stiffness values when compared to other values in the literature (table 2). Moreover the prototype carbon fibre swingarm is 1.5 kg lighter than its aluminium counterpart: a weight saving of 29%.

5.3 Strain measurements

The applied loads simulated typical loads: the aim was not to apply loads to failure. The aim with both the deflection and strain measurements was to obtain the stiffness and strain characteristics of the swingarm. The strain measurements gave an indication of the following: (1) where the maximum strains occur (2) the relative strain values and (3) whether the strains are tensile or compressive.

Figure 17 shows that the maximum tensile and compressive longitudinal strains due to vertical loading occur at Positions 5 (1100 με) and 4 (-1100 με) respectively. The maximum tensile and compressive transverse strains (figure 18) were measured at Positions 3 (850 με) and 5 (-900 με) respectively. Under the maximum vertical loading of 8000 N, the maximum tensile and compressive strains were well below the ultimate tensile and compressive strains of 8000 με[17].

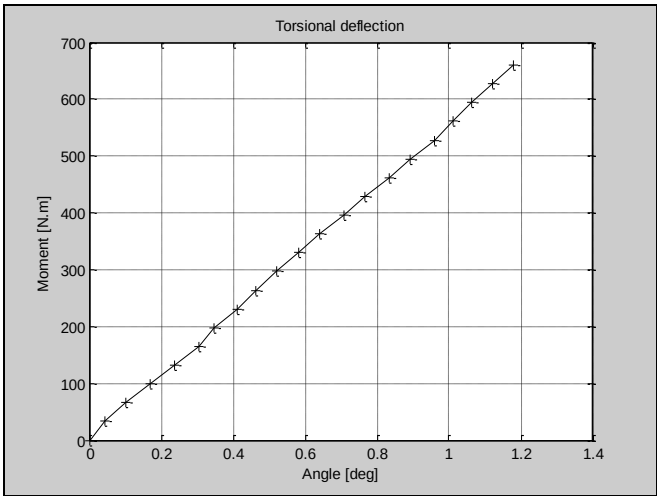


Figure 16: Torsional deflection

Table 1: Comparison of torsional stiffness values

Designation	**Torsional stiffness (Nm/deg)**
Kawasaki ZX10R[10]	102.9
Suzuki GSX R1000[10]	140.8
Honda CBR 1000R[10]	140.8
Sharp[12]	209
Ducati Carbon Fibre (this study)	550
S2008[7]	670
SM 2008[7]	890
BNG 2008[7]	1330
Cossalter[13]	1000 - 2000

The normalised strains on the top arm due to vertical loading are shown in table 3. The results suggest that under increased vertical loading conditions, Position 5 is likely to experience failure first due to experiencing the highest strains.

Table 2: Normalised strain on the top arm of the swingarm during vertical loading

Position	Longitudinal	Transverse
4	-1	0.64
5	1	-0.81
6	0.68	-0.36

The fibre layup on the swingarm was a symmetrical design made up of a number of unidirectional and weave (0-90°) plies. Therefore the longitudinal and transverse directions have the same strain to failure.

The longitudinal and transverse strains from torsional loading are shown in figures 19 and 20. Position 6 undergoes the highest longitudinal tensile strain (380 με) and Positions 5 and 6 experience the highest transverse compressive strain (250 με).

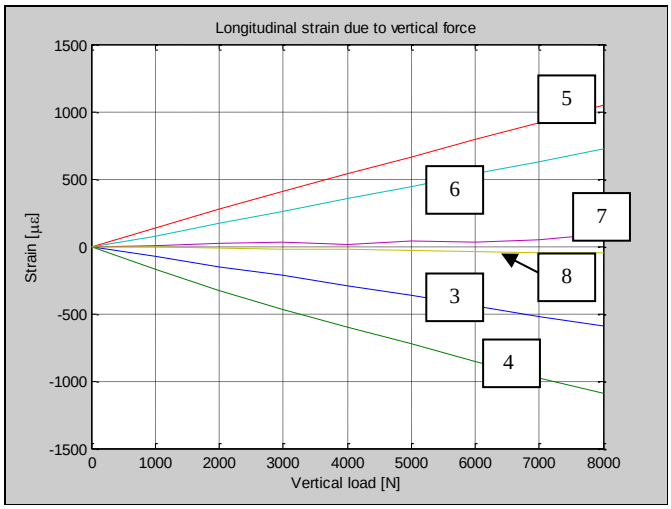


Figure 17: Longitudinal strain measured during vertical loading

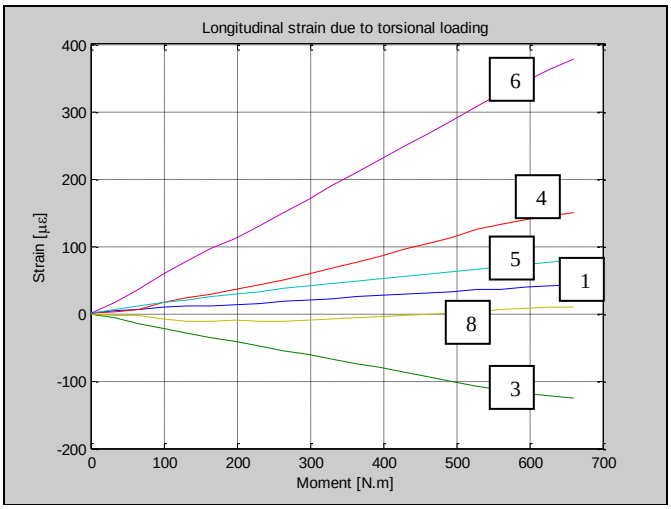


Figure 19: Longitudinal strain measured during torsional loading

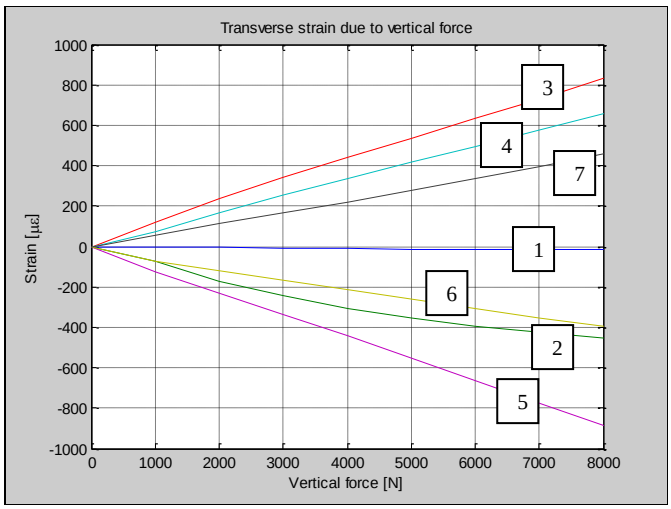


Figure 18: Transverse strain measured during vertical loading

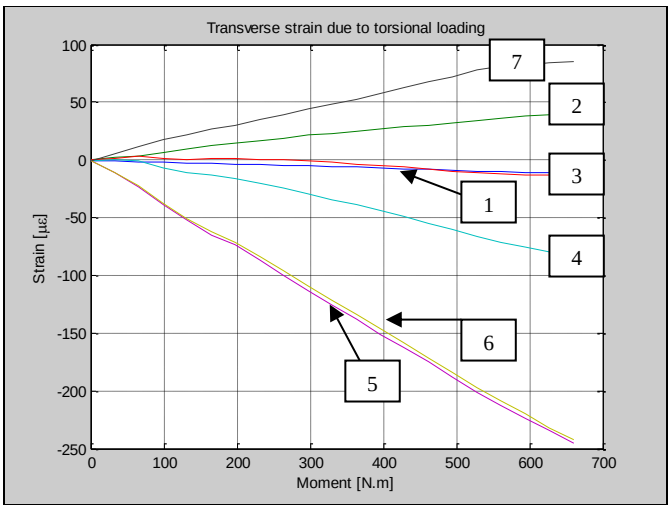


Figure 20: Transverse strain measured during torsional loading

Table 4 shows the normalised strain on the top arm which suggests that Position 6 is a limiting position during torsional loading i.e. it will tend to fail first as the torsional load is increased.

Table 3: Normalised strain on the top arm of the swingarm during torsional loading

Position	Longitudinal	Transverse
4	0.39	-0.21
5	0.21	-0.65
6	1	-0.65

6 FE results and discussion

The following section compares the FE and experimental results. Major challenges were encountered in validating the FE model of the carbon fibre swingarm. As discussed earlier, due to the complexity of the swingarm, the modelling of ply overlap all over the structure proved to be highly difficult and an FE model was developed where the plies were modelled using butt joints. The following therefore presents the results using this modelling technique.

6.1 Deflections

The differences between the FE and experimental deflections were 5% (vertical) and 28% (torsional). The reason for the large difference in the torsional deflections is explained by the FE model not including ply overlap. In the FE results that follow, the longitudinal results are relatively accurate but the results depending on the transverse properties of the laminate are less accurate; which is consistent with the explanation of the less accurate torsional deflection results.

6.2 Strains

The experimental tests showed that the highest strains occurred on the top arm: Positions 4 and 5 (figure 21) and Position 6 (figure 22). The following therefore compares the FE strains on the top arm with the experimental results during vertical loading. Three positions on the top arm were analysed in their respective longitudinal and transverse directions.

Position 4 in the longitudinal direction showed good correlation (1% error) (figures 23 and 24). The experimental strain at the maximum load of 8000 N was measured as -1090 με and the FE strain was calculated as −1100 με.

The strain at Position 4 in the transverse direction did not produce good correlation (figures 25 and 26). The FE strain at 8000 N was 1700 με compared with experimental strain of 660 με, a difference of 157%. This large difference is attributed to the lack of ply overlap in the FE model in this area and due to the high strain gradient where the strain was measured. In an attempt to simulate the ply overlap, extra plies were added to the area surrounding Position 4. The plies at Position 4 consist mainly of ±45° woven laminas. Three extra ±45° woven plies were added and new longitudinal and transverse strains were calculated. The FE longitudinal strain was minimally affected by the extra plies: the new longitudinal strain was found to be -1050 με which is not significantly different from the original -1100 με. The transverse direction however, was significantly changed by the addition of the three plies: the new transverse strain was calculated to be 1000 με which shows a decrease of 700 με and a new difference of 40% when compared with the experimental results. This exercise shows that simply by adding three plies to simulate overlap, the transverse strain becomes significantly more accurate and the longitudinal strain remains almost the same. The overlap plays a huge role in obtaining accurate transverse FE strain results but minimally affects the longitudinal strain. It is concluded that to accurately model the swingarm at Position 4 the ply overlap must be included in the model.

Position 5 in the longitudinal direction showed good correlation (difference = 5%). The experimental strain due to the vertical load of 8000 N was 1050 με compared with the FE strain of 1100 με (figures 27 and 28). This longitudinal strain result together with the longitudinal strain result at Position 4, indicate that good correlation is found in the longitudinal direction.

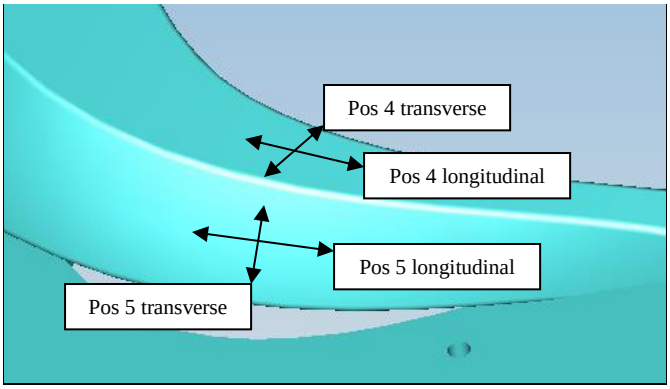


Figure 21: Top arm showing longitudinal and transverse directions of Positions 4 and 5

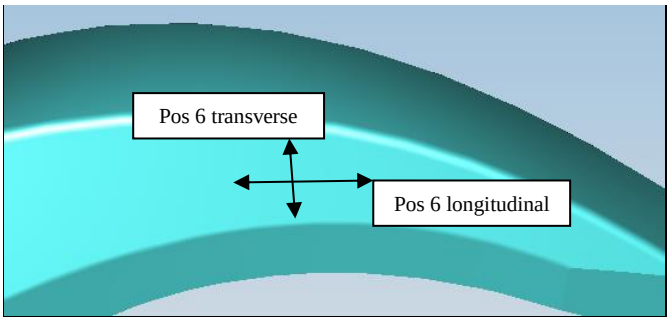


Figure 22: Underside of top arm showing longitudinal and transverse directions of Position 6

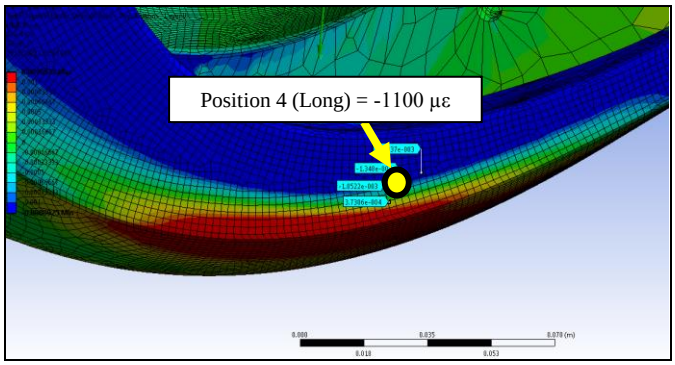


Figure 23: FE results at Position 4 in the longitudinal direction at 8000 N

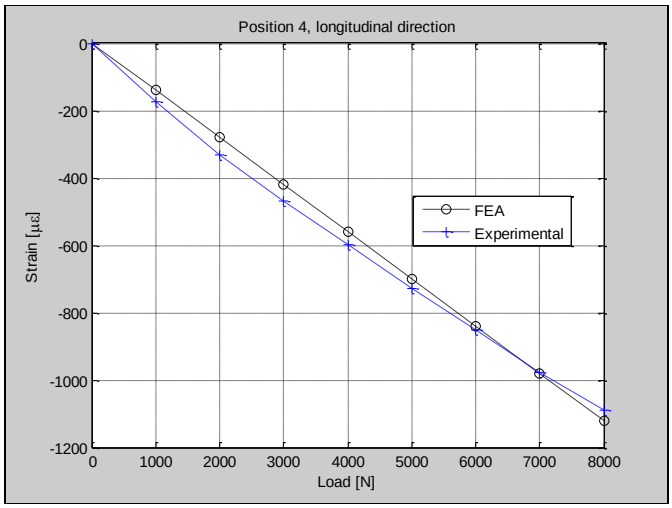


Figure 24: Comparison between FE and experimental strain at Position 4 in the longitudinal direction

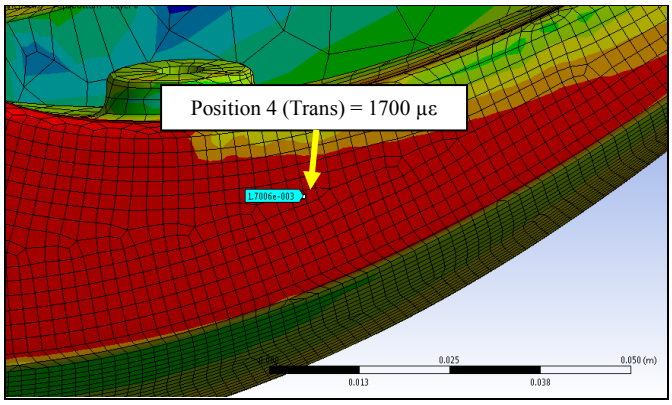


Figure 25: FE results at Position 4 in the transverse direction at load of 8000 N

The transverse strain at Position 5 was calculated as -1200 με and gives an error of 38% when compared with the experimental value of -870 με (figures 29 and 30).

However, viewing the results approximately 10 mm above Position 5 (figure 29), a strain of -840 με is found on the FE model which is near to the measured value of -870 με. This suggests that the simulated load paths are slightly different to the actual load path due to different rigidity in the transverse direction.

The FE strain at Position 6 in the longitudinal direction was calculated as 1000 με (figure 31) and a difference of 38% is found when compared with the experimental strain

of 725 με (figure 32). Although a large difference of 38% was calculated for Position 6 in the longitudinal direction, the longitudinal strain 10 mm above Position 6 was found to be 730 με which is near to the measured strain. The difference can again be attributed to the lack of ply overlap which causes the load paths to change slightly.

The strain at Position 6 in the transverse direction was calculated as -830 με (figure 33). A difference of 110% was calculated when compared with the experimental value of -394 με. The difference is unacceptably high but the strain 10 mm below Position 6 was found to be -400 με which is within 2% of the measured value. To see the effect of ply overlap has on this region, three ±45° woven plies were added and the new transverse strain was calculated as -400 με which is within 2% of the measured value. Once again, the importance of ply overlap is evident.

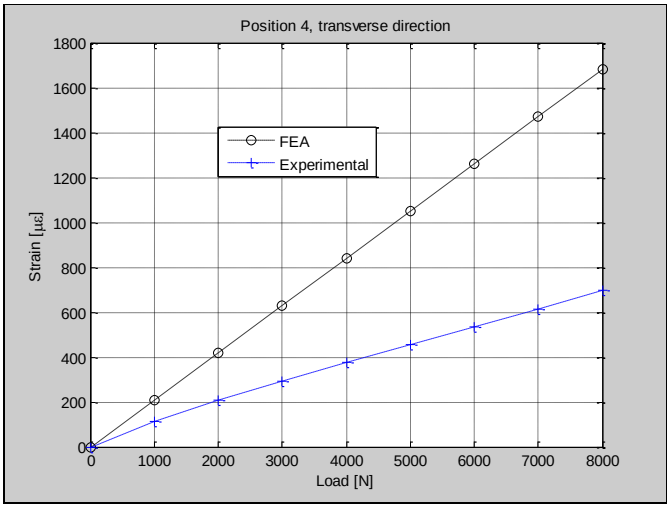


Figure 26: Comparison between FE and experimental results at Position 4 in the transverse directions

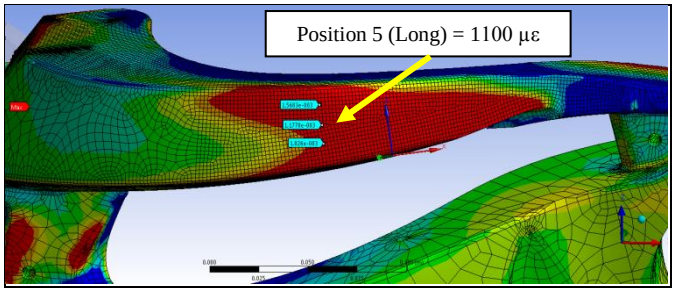


Figure 27: Longitudinal strain at Position 5 under vertical load of 8000 N

7 Conclusions

A prototype carbon fibre swingarm was presented in this paper highlighting (1) the importance of determining the swingarm stiffness and (2) the challenges involved with developing an accurate composite FE model for highly complex geometries such as the swingarm in this study. The swingarm stiffness influences the weave mode stability of the motorcycle and therefore is an important characteristic. The vertical stiffness was found to be an order of magnitude higher than the motorcycle rear spring stiffness which suggests the vertical stiffness is sufficiently high. The measured swingarm torsional stiffness is of comparable torsional stiffness to those published in the literature. Moreover the prototype carbon fibre swingarm is 1.5 kg lighter than its aluminium counterpart: a weight saving of 29%.

The maximum strains measured were found to be significantly lower than the maximum allowable strains in tension and compression. This indicates the strength of the swingarm is sufficient.

A FE model was developed with mixed results. In terms of deflections, differences between numerical and experimental results were found to be 4% and 28% for the vertical and torsional deflections respectively. Differences in strain on the top arm of the swingarm were found to be satisfactory (less than 10%) and unsatisfactory (larger than 100%). The large differences were attributed to the complicated geometry of the swingarm which did not facilitate the modelling of ply overlap. Ply overlap was approximated by adding plies to certain areas which resulted in significant improvements in the results when compared with the experimental values.

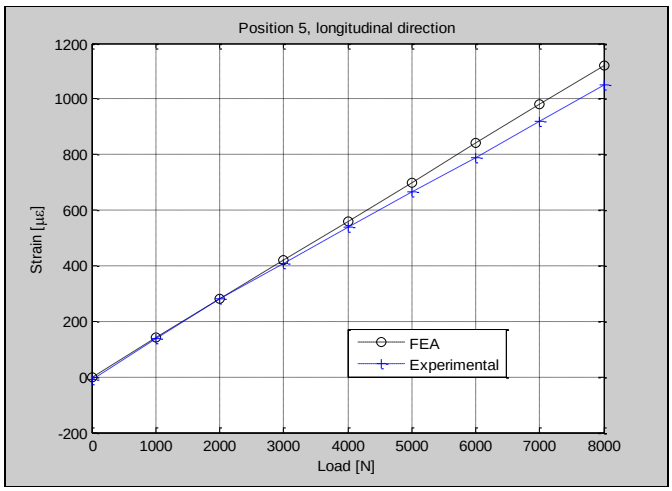


Figure 28: Comparison between FE and experimental strain at Position 5 in the longitudinal direction

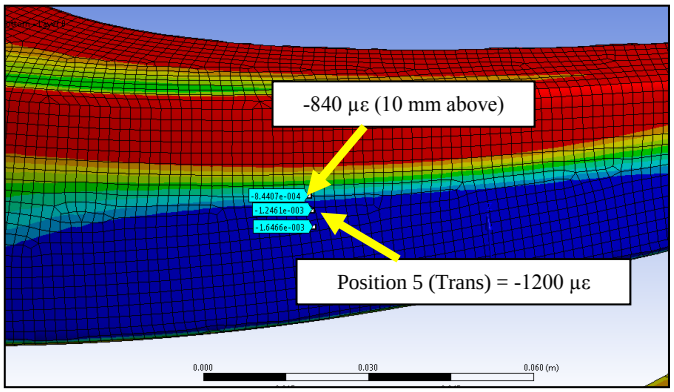


Figure 29: Strain distribution at Position 5 in the transverse direction

Acknowledgements

This work is based on the research supported in part by the National Research Foundation of South Africa (TP13082630765 Light, Strong, High Performance Automotive Product Development). The grantholder acknowledges that opinions, findings and conclusions or

recommendations expressed in any publication generated by the NRF supported research are that of the authors and that the NRF accepts no liability whatsoever in this regard. The authors gratefully acknowledge the support of BlackStone Tek who collaborated with the development of the test rig and prepared the prototype swingarm. Without their support this research would not have been possible.

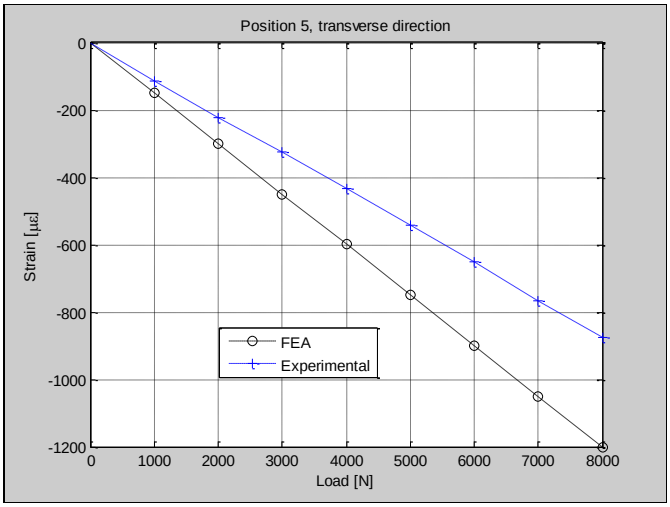


Figure 30: Comparison between FE and experimental strain at Position 5 in the transverse direction

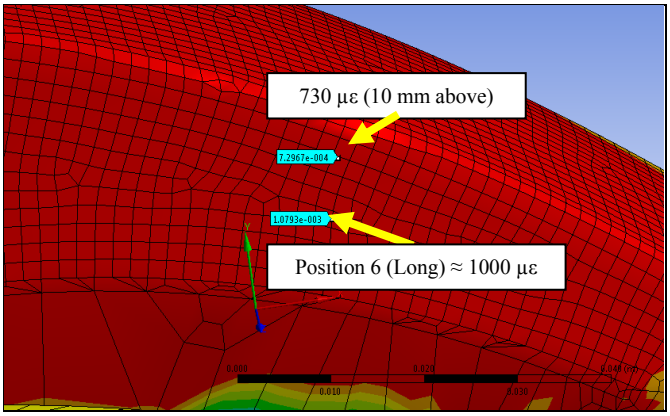


Figure 31: Strain distribution for Position 6 in the longitudinal direction

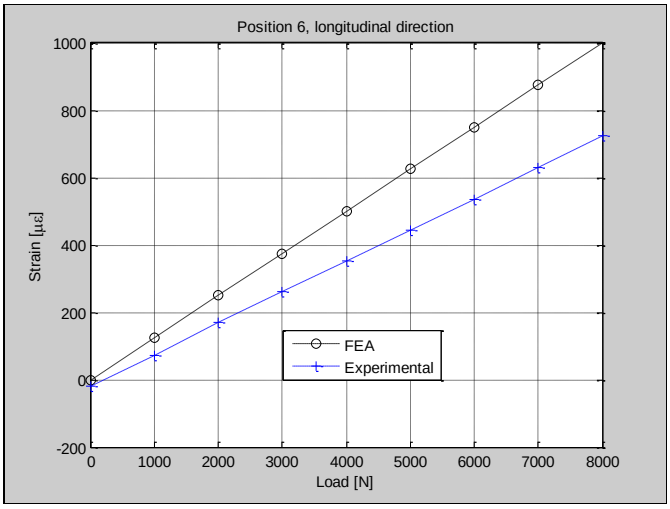


Figure 32: Comparison between FE and experimental strain at Position 6 in the longitudinal direction

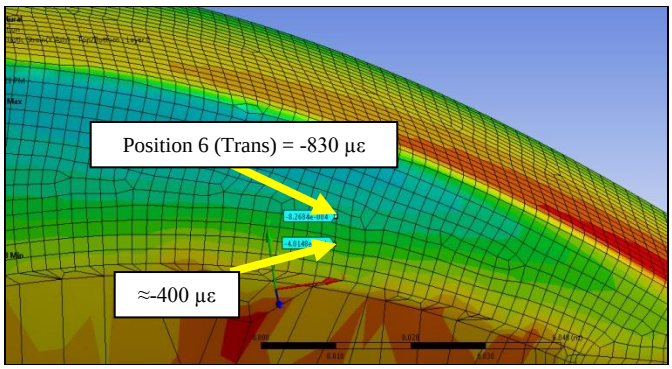


Figure 33: Strain distribution at Position 6 in the transverse direction

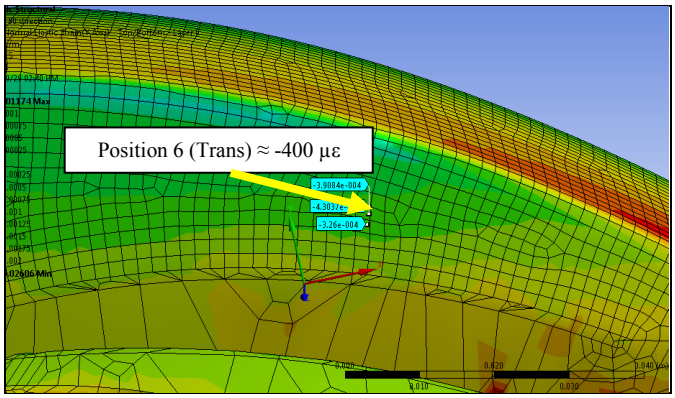


Figure 34: Transverse strain at Position 6 after adding three ±45° woven plies

References

1. *Adam H*, Carbon Fibre in Automotive Applications, *Materials & Design*, 1997, 18(4), 349-355.
2. *Turner TA, Harper LT, Warrior NA and Rudd CD*, Low-cost Carbon-fibre-based Automotive Body Panel Aystems: A Performance and Manufacturing Cost Comparison, *Proceedings of the Institution of Mechanical Engineers, Part D: Journal of Automobile Engineering*, 2008, 222(1), 53-63.
3. *Kim D-H, Choi D-H and Kim H-S*, Design Optimization of a Carbon Fiber Reinforced Composite Automotive Lower Arm, *Composites Part B: Engineering*, 2014, 58, 400-407.
4. *O'Dea N*, Motorcycle Swingarm Redesigned in Carbon Composite, *Reinforced Plastics*, 2011, 55(6), 38-41.
5. *Dragoni E and Foresti F*, Design of a Single-sided Composite Swingarm for Racing Motorcycles, *International Journal of Materials and Product Technology*, 1998, 13(3), 411-420.
6. *Airoldi A, Bertoli S, Lanzi L, Sirna M and Sala G*, Design of a Motorcycle Composite Swing-arm by Means of Multi-objective Optimisation, *Applied Composite Materials*, 2012, 19(3-4), 599-618.
7. *Risitano G, Scappaticci L, Grimaldi C and Mariani F*, Analysis of the Structural Behavior of Racing Motorcycle Swingarms, *SAE Technical Paper*, 2012, 2012-01-0207.
8. *Cassani S and Mancuso A*, Shape Optimization of a High Performance Motorbike Single Sided Swingarm, *SAE Technical Paper*, 2005, 2005-01-0887.

9. *Cossalter V, Lot R and Massaro M*, The Influence of Frame Compliance and Rider Mobility on the Scooter Stability, *Vehicle System Dynamics*, 2007, 45(4), 313-326.
10. *Armentani E, Fusco S and Pirozzi M*, Numerical Evaluation and Experimental Test for a Road Bike Swingarm, *JUMV International Automotive Conference with Exhibition*, April, Beograd, Serbia, 2007.
11. *Lake K, Thomas R and Williams O*, The Influence of Compliant Chassis Components on Motorcycle Dynamics: An Historical Overview and the Potential Future Impact of Carbon Fibre, *Vehicle System Dynamics*, 2012, 50(7), 1043-1052.
12. *Sharp RS*, The Influence of Frame Flexibility on the Lateral Stability of Motorcycles, *Journal of Mechanical Engineering Science*, 1974, 16(2), 117-120.
13. *Cossalter V*, Motorcycle Dynamics, Lulu.com, 2006.
14. *Stan C*, Development Trends of Motorcycles II, Germany: Expert Verlag, 2005.
15. *Iwasaki H, Mizuta A, Hasegawa T and Yoshitake H*, Development of a Magnesium Swing Arm for Motorcycles, *SAE Technical Paper*, 2004, 2004-32-0048.
16. *Hoksbergen JS, Ramalu M, Reinhall P and Briggs TM*, A Comparison of the Vibration Characteristics of Carbon Fiber Reinforced Plastic Plates with those of Magnesium Plates, *Applied Composite Materials*, 2009, 16(5), 263-283.
17. *Limited Performance Composites*, Mechanical Properties of Carbon Fibre Composite Materials, Fibre/Epoxy resin (120°C Cure), Performance Composites Limited, 2009, http://www.performance-composites.com/carbonfibre/mechanicalproperties_2.asp, 2013.

 © SAIMechE All rights reserved.